

The non-trivial magnetic configuration in neutron stars

Daniele Viganò 

Institute of Space Sciences (IEEC-CSIC), E-08193 Barcelona, Spain;

Institut d'Estudis Espacials de Catalunya (IEEC), 08034 Barcelona, Spain;

Institut d'Aplicacions Computacionals de Codi Comunitari (IAC3), Universitat de les Illes Balears, Palma de Mallorca, Balears E-07122, Spain;

email: vigano@ice.csic.es

Abstract. While predominantly dipolar, large-scale magnetic fields are usually assumed in most studies involving neutron stars, there are multiple observational, theoretical hints and numerical simulations highlighting the importance of non-dipolar components. I review here the most important observational facts and numerical studies pointing towards the existence of magnetospheric currents and internal small-scale structures, arising from multipoles of poloidal and toroidal fields. This holds for all neutron star stages: at birth, during their lifetime and after a merger.

Keywords. MHD, Magnetic fields, stars:neutron, stars: pulsars, gravitation, radiation mechanisms: thermal

1. Magnetism in astrophysical bodies

When magnetic fields are related to neutron stars (and to astrophysical objects in general), the collective imagination often pictures a simple dipole. While this is an acceptable zero-order approximation, useful for some estimations, both observations and magneto-hydro-dynamics (MHD) theory suggest that nature tends to lead to much more complex topologies.

The only firm empirical, direct measurements of the magnetic topology in astrophysical objects come from the magnetograms of the Sun (see e.g. the classical reviews [Stenflo \(1978\)](#); [Solanki \(1993\)](#)), the in-situ measurement of solar planets (the Earth ([Lowes \(1974\)](#)) and Jupiter ([Connerney et al. \(2018\)](#)) in much more detail than others), and the Zeeman-Doppler mapping of main sequence stars (e.g., [Kochukhov \(2016\)](#)). In all these cases, at the surface the magnetic field \vec{B} is much more complex than a dipole, showing a continuous distribution of magnetic energy over different spatial scales, and non-potential configurations (i.e., $\vec{\nabla} \times \vec{B} \neq 0$) due to the presence of electrical currents and/or winds. The celestial bodies that seem to show the closest resemblance with a magnetic dipole could be the Ap/Bp stars (see [Aurière et al. \(2007\)](#) for a discussion about the magnetism dichotomy in main-sequence stars), even though refined observations challenge this view ([Kochukhov et al. \(2022\)](#)). In other words, small magnetic structures, magnetospheric currents and/or winds seem ubiquitous in magnetized astrophysical bodies. Only if winds are not strong enough to stretch and twist the field lines (as in main-sequence stars and fast-rotating objects), the dipolar component can clearly dominate far above the surface.

Compared to the continuous dynamo operating in main-sequence stars and planets, the magnetism in neutron stars and white dwarfs is radically different. Moreover, it can

be inferred only indirectly, mainly by spinning properties or interpretation of spectral features. Their magnetic fields are generated at birth (by flux conservation and MHD amplification mechanisms), after which they basically decay due to Ohmic dissipation and slowly re-organize themselves under different MHD effects. Despite the striking differences between these astrophysical objects, similar processes (convection, differential rotation) that sustain the stellar and planetary dynamos operate in the processes leading to the natal magnetic field amplification in neutron stars (on which we focus hereafter): one should also expect a non-trivial topology at birth for them.

It is then not a surprise to see an increasing amount of observational hints for the presence of a complex topology in different classes of neutron stars, especially for the most magnetized ones, the so-called magnetars (see e.g. (Esposito et al. (2021)) and A. Borghese's contribution in this volume). In the last decade several pieces of evidence seem to confirm the idea, exposed in the very first magnetar models (Thompson & Duncan (1993)), that they cannot be characterized by a simple dipole. The internal topology should be much richer. I give a brief overview of such observational evidences in the next section, relating in particular what we can learn about topology from the persistent and transient thermal emission of magnetars. Then, I will discuss how the magnetic topological complexity is a constant feature throughout the neutron star's life, including birth and binary neutron star mergers.

2. Observational evidences

2.1. Pulsars and magnetars' persistent emission

Persistent X-ray emission from different kinds of neutron stars shows complementary evidences for a non-dipolar topology.

First, NICER data from millisecond pulsars provide X-ray light curves which seem to indicate a complex temperature map incompatible with a dipolar, symmetric configuration (Riley et al. (2019); Bilous et al. (2019)). A reverse-engineering exercise is needed in order to find which temperature map distributions are compatible with the observed light curves in specific energy ranges. The problem is substantially degenerate, because of the restricted energy range (limited by absorption at \lesssim few keV) and the huge space of parameters, containing both geometrical angles and a potentially infinite number of possible surface temperature distribution. Despite these caveats, the Bayesian inference analysis on NICER data calls for a non-antipodal configuration of the X-ray emitting hotspots. The temperature map is shaped from inside by the anisotropic thermal conductivity induced by the intense magnetic fields (e.g., Potekhin et al. (2015)). The subsequently inferred non-antipodality of the magnetic field is in line with the asymmetries usually found also in planets and stars, and is the outcome of the non-trivial birth and evolved magnetic topology.

Secondly, small-scale structures are invoked to explain the spectral features seen in at least one magnetar (Tiengo et al. 2013) and in a couple of the nearby thermally emitting neutron stars (Borghese et al. 2015, 2017). These features are interpreted as resonant Compton absorption between thermal surface photons and relatively dense plasma contained in coronal loops, although specific surface temperature inhomogeneities (again associated to internal, non-trivial magnetic fields) could give similar effects in some cases (Viganò et al. (2014)).

Thirdly, most magnetars show soft X-ray non-thermal components (\lesssim 10 keV). Moreover, many persistent magnetars also show a hard X-ray tail (\sim 20 – 200 keV) in quiescence (e.g., Götz et al. (2006)). The soft non-thermal contribution is well explained by the resonant Compton up-scattering of photons by dense plasma (Rea et al. (2008)). The inferred plasma density is orders of magnitude larger than the value that one would

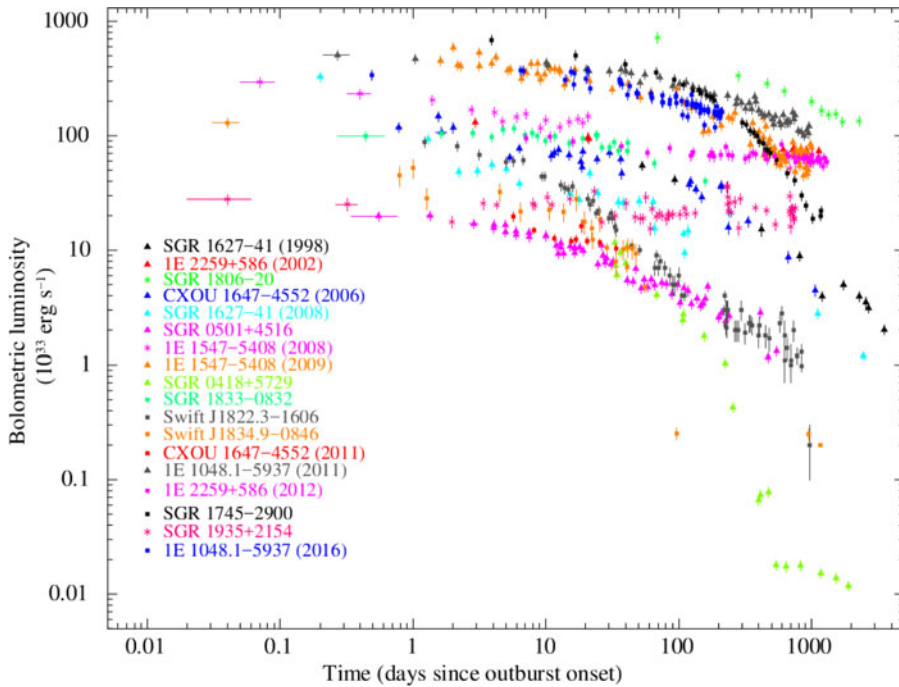


Figure 1. Summary of 0.01-100 keV luminosity evolution during the known outbursts, taken from Coti Zelati et al. (2018).

expect from a simple rotating dipole (Goldreich & Julian (1969)), and is consistent with the presence of charged particles persistently flowing in localized loops close to the surface (a few stellar radii), qualitatively similar to the Solar prominences and filaments. The same magnetospheric currents would then be responsible for the hard X-ray tails, via acceleration of particles along the loops (Beloborodov (2013); Wadiasingh et al. (2018)) at higher altitudes above the surface. The presence of strong, persistent currents in the closed magnetosphere necessarily implies a deviation from a rotating dipole, and indicates multipolar, non-potential structures emerging from the surface.

Fourth, and related to the previous point, a pretty common feature of magnetars thermal spectra is the rather small size ($\sim \text{km}^2$ or less) of the inferred emitting hotspots. On one side, the quiescent bolometric thermal luminosity and timing properties of thermally emitting neutron stars can be explained pretty well by the diffusion of the heat produced by the electrical currents circulating in the crust (Viganò et al. (2013)), with variations given by the initial field and age. However, on the other side, the synthetic spectra arising from such theoretical surface temperature maps show an inferred radius of at least a few km, larger than what shown by many magnetars. Within standard magneto-thermal models, smaller apparent hotspots can be originated only by concentration of magnetic fields due to the evolution of quite extreme, ad-hoc, initial internal topologies (Geppert & Viganò (2014)), or more likely, by the dissipation at the surface of the magnetic (and kinetic?) energy associated to the electrical currents flowing along the loops. In either case, a pure dipole is inconsistent with results from observations: the thermal and non-thermal spectra strongly point to the presence of non-trivial magnetic fields both in the magnetosphere and in the interior.

2.2. Magnetars outbursts: internal and external scenarios

Additional evidences come from the precious data of the ~ 20 magnetar outbursts detected and followed up so far (see [Coti Zelati et al. \(2018\)](#) for a review and A. Borghese's contribution in this volume). A typical outburst consists in an enhancement of the flux, reaching X-ray luminosities up to few times 10^{35} erg s $^{-1}$, and then a decay in timescales that can range from months to some years (see [Fig. 1](#)). Outbursts are a fundamental tool to detect new magnetars, especially when their pre-outburst level is too low to have been detected by surveys or other observations. Among the magnetars discovered during the *Fermi* and *Swift* era (~ 1 per year), the so-called low-B magnetars (e.g., [Rea et al. \(2010\)](#); [Rea et al. \(2012, 2014\)](#)) are very interesting, since their timing properties suggest a dipolar field in the range of normal pulsars. However, the fact that they show magnetar-like transient activity requires that the average crustal magnetic field intensity needed to support the transient emission is much larger than the timing-inferred value of the dipole. This supports the idea of non-trivial internal and external topologies. Note that, usually, a simplified version of non-trivial topology refers to “strong toroidal fields”, having in mind large-scale, axisymmetric torus shape on top of the dipole. However, as we will see below, realistic topologies are more complex, having a range of small and large spatial scales in both the poloidal and toroidal components. When mentioning the effects of non-trivial configurations, it would be more correct to refer them more generally as “internal, non-dipolar” fields.

Going back to the standard interpretation of outbursts, the pre-outburst state is dubbed as quiescent, and is usually thought to correspond to the surface temperature map given by the coupled secular cooling and magnetic evolution since birth (magneto-thermal evolution). Such long-term evolution happens in timescales of thousands of years or more, thus astronomically unobservable. The evolving magnetic fields may become sporadically unstable, and this may happen in two ways. One is in the magnetosphere as a consequence of a slow twisting of lines from inside due to the Hall and Ohmic dynamics (see below for the evolution models), and we will call this a magnetospheric trigger hereafter. The other, more popular, relies on a sudden failure of the crust, triggered by an excess of magnetic stress (see e.g. [Pons & Perna \(2011\)](#); [Perna & Pons \(2011\)](#); [Dehman et al. \(2020\)](#); [Kojima et al. \(2022\)](#)), causing an instability that launches thermo-plastic waves ([Beloborodov & Levin \(2014\)](#); [Li et al. \(2016\)](#); [Thompson et al. \(2017\)](#)) and propagates to the magnetosphere, injecting helicity into it. In either case, the instability is accompanied by the deposition of heat at the surface, from either inside or outside, naively sketched in [Fig. 1](#).

Deposition from inside. In internal cooling models, the heat is suddenly released in the crust due to dissipation of mechanical energy ([Pons & Rea \(2012\)](#)). Part of this heat diffuses towards the surface, while part of it is released in neutrino emission in deep layers. The deeper the deposition, the less efficient is the propagation of heat to the surface. This simple scenario, originally studied in low-mass X-ray binaries (e.g., [Cumming & Macbeth \(2004\)](#)) has been studied quantitatively in detail for many cases (see e.g. [Rea et al. \(2012\)](#)), and its signatures are: (i) a flux decay timescale of months, a few years at most; (ii) a temperature that cannot be kept higher than ~ 0.3 keV for more than ~ 1 year; (iii) an emitting radius (associated to the hotspot) that, being created by diffusion, gets larger in time, or at most remains roughly constant if it is magnetically confined.

Deposition from outside. An alternative is the external heating model, for which magnetospheric, nearly force-free currents circulate, due to the dynamical nature of the internal field that feeds them by helicity injection. The electrical loops close inside the outermost layer of the crust and have to pass through the very resistive envelope (see

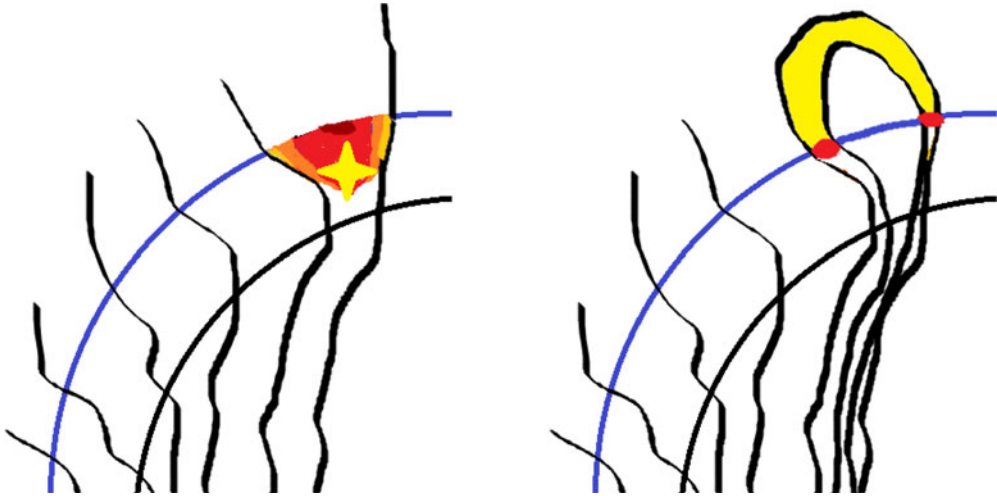


Figure 2. Cartoon sketch about the internal (left) or external (right) scenario leading to the formation of surface hotspots (red colors) during an outburst. In the internal scenario, the deposition of heat at some depth (yellow) propagates to the surface. In the external scenario, the magnetospheric currents (yellow) close inside the star and dissipate energy at their surface footprints. (Note: the magnetic field topology drawn here with black lines has no particular meaning.)

Karageorgopoulos et al. (2019) for a quantitative simulation of current closure in the case of the open field lines of a standard pulsar). This causes a strong localized Joule dissipation that can heat up the surface to \sim keV relatively easily (Akgün et al. (2018)). The expected size of the emitting region corresponds to the size of the loop footprints, it is theoretically unconstrained but can potentially be as small as the observationally inferred values. This scenario (Beloborodov & Thompson (2007); Beloborodov (2009, 2011, 2012)) suffers from intrinsic large uncertainties, but the basic predictions are: (i) shrinking emitting radii with time; (ii) timescales of the existence of such loops (or j -bundles) ranging from months to decades (Beloborodov (2009); Coti Zelati et al. (2020)) depending on the extension of the loop and on poorly known magnetospheric impedance, among other uncertainties.

In fact, observations point to a shrinking of the emitting surface in time in most cases, and temperatures that in several cases are kept too high to be maintained from internal diffusion. This seems to favor the magnetospheric dynamics as the dominant source of surface heating, at least in many cases. See also Beloborodov & Li (2016) for a review about magnetar heating mechanisms.

In both cases, the temperature and emitting radius should eventually go back to the pre-outburst state, but in different timescales. Let us compare with observations. For the (not many) magnetars with a good measurement of the pre-outburst emission, the post-outburst flux indeed tends to relax to the pre-outburst one in several cases, enforcing the idea of a quiescent state (Coti Zelati et al. (2018)). However, at least a couple of cases stand out for the peculiar post-outburst behaviour. On one side, the well-known magnetar 1E 1547.0-5408, that went outburst in 2008 and 2009, has apparently never recovered the low pre-outburst flux (see Fig. 3 taken from Coti Zelati et al. (2020)). Instead, in the last years it seems to have stabilized its flux to a value 20 times larger than before. Another exceptionally slow decay is the one of SGR J1745-2900, a magnetar tightly bound to the Galactic center (Rea et al. 2013), showing a new quiescent level below the pre-outburst one (Rea et al. 2020). Other magnetars could show a similar

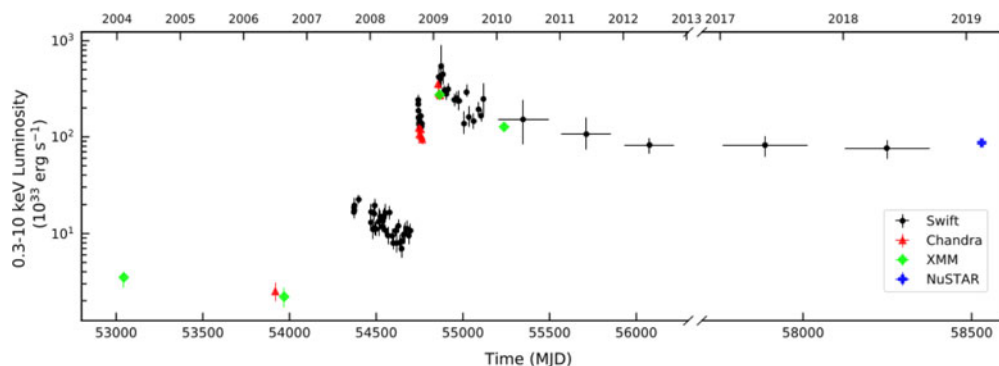


Figure 3. The peculiar change of persistent state of AXP 1E1547.0-5408 between before and after the 2008-2009 outbursts event. Taken from [Coti Zelati et al. \(2020\)](#).

behaviour (possibly, [Younes et al. \(2017\)](#)), but the lack of good pre-outburst data or the large distance/absorption prevent us from any clear assessment.

Therefore, does the quiescent state really exist? The easier explanation to the change of the so-called quiescent state in 1E 1547.0-5408 invokes a drastic change of the thermal map at the surface and of the non-thermal magnetospheric contribution. In order to shed light on this, let us revisit our recently performed force-free, general relativistic 3D simulations of the magnetospheric dynamics, responding to non-axisymmetric twists of spots [Carrasco et al. \(2019\)](#). We followed the injection of twist from arbitrarily located spots, and evaluate the currents impacting on the surface, and the consequent thermal emission due to the high resistivity of the external layers of the envelope ([Akgün et al. 2018](#)). What we found is that the hotspot temperature increases with the twist injection, reaching a maximum just before the re-organization of the magnetic field. After the reconnection, the system relaxes to a new state with dynamically stable, non-zero electrical currents. The inferred temperature after the event is slightly smaller than the maximum reached just before. How is this constraining any outburst model? We know from observations that the pre-outburst values of temperature and flux (or their upper limits) are in general much smaller than the post-outburst ones. The two closest-to-outburst quiescent states serendipitously measured were less than two days the events ([Esposito et al. 2008](#); [Younes et al. 2017](#)). As a consequence, the twist injection has to be much faster than \sim day (as pointed out in [Younes et al. \(2017\)](#) as well), compatible with having happened in much shorter (Alfvén) timescales, otherwise we would see a secular change of temperature before the events, and little difference between before and after the event.

The conclusion is that the outbursts are not caused directly by a magnetospheric trigger, but by a crustal instability that then propagates outside. Moreover, our study found that the post-outburst configuration was different from the initial one (a simple dipole). Such new system of currents persists at least over the dynamical (Alfvén) timescales there simulated, giving the idea that outbursts may be accompanied by a reconfiguration of a stable, slowly decaying current system, and, therefore of the thermal and non-thermal persistent emission, like the ones observed in 1E 1547.0-5408. The contribution from such currents co-exist with the thermal flux coming from the secular cooling, and one may dominate over the other depending on how much currents flow around a given neutron star.

3. Complex magnetic fields throughout neutron star's life

3.1. Birth

During the supernova collapse, the average magnetic field intensity of the progenitor star gets amplified. On one side, the magnetic flux conservation acts: as the core shrinks, it drags and concentrate the magnetic field lines. On the other side, the convection and differential rotation that characterize the latest stages of the collapse can amplify the field (Thompson & Duncan 1993) via, arguably, convective instability (Miralles et al. 2000), magneto-rotational instability (Reboul-Salze et al. 2021a,b) and precession (Lander 2021).

How does the magnetic field look like once the proto-neutron star phase is terminated? There are two main ways to study it. The one that prevailed until a few years ago was to study some possible equilibrium states. There is a long series of works by different groups about this (e.g., Ciolfi et al. (2009); Lander & Jones (2009); Ciolfi & Rezzolla (2013); Lander et al. (2021)), and virtually all of them rely on looking for MHD equilibria, assuming a dipole-like topology for the poloidal field (or in any case large-scale, limited to the first multipoles), and enforcing a matching with a perfect potential solution outside. The outcome of these simulations is the so-called twisted torus topology, a very smooth, configuration resembling at large scales what found in the pioneering studies for main sequence Ap stars (Braithwaite & Spruit 2004; Braithwaite & Nordlund 2006).

Note that, in these “static” searches of MHD equilibria, the topological (axial symmetry, initial dipolar field) and boundary assumptions (vacuum solution) strongly determine the equilibrium topology found at the end of the numerical process, by construction. In this sense, the solutions are not unique, as it can be seen when different multipoles are considered (Ciolfi et al. 2009). These solutions can give a broad picture of the large-scale topology but are not saying much about the small-scale structures.

On the other side, there has been huge progress in long MHD simulations of core-collapse supernovae (Mösta et al. 2015; Reboul-Salze et al. 2021a,b). These recent results provide a more complex picture, where magnetic energy is spread across all the scales, with a magnetic energy spectrum that clearly looks turbulent. Only a minor fraction ($\sim 5\%$) of the total magnetic energy is stored in the dipolar component. This seems compatible with complementary MHD studies of hot neutron stars, which find (again with strong assumption at the outer boundary) the presence of multipolar structures (Sur et al. 2020), alongside the classical twisted torus.

A widespread argument to neglect the small scales is that the magnetic energy contained therein would be quickly washed away by the resistivity. This is certainly true for structures having size similar to the resistive scale, and will have the effect of steepening the magnetic spectra. However, one should expect that, hours after birth (when a non-negligible portion of the crust has formed), only the tail of the proton-neutron star's magnetic spectrum would have been filtered, leaving the magnetic energy still stored in a broad range of scales, being the large-scale components a minor fraction of the total. This is actually what already predicted by the first magnetar models Thompson & Duncan (1993): a dominion of sub-km scale magnetic structures.

3.2. Long-term evolution of the magnetic field in the crust

After the crust is formed by freezing (minutes to months to approach its final size), the magnetic field starts to evolve. There are no relevant processes injecting further magnetic energy in the system, but the electrically conducting species in the interior keep moving, providing the secularly-evolving currents that sustain the magnetic field.

The MHD regulating the solid crust of the neutron stars is fairly understood (Pons & Viganò 2019). In this case the induction equation is derived by the so-called

Hall–MHD (or electron–MHD) approximation, according to which ions are completely fixed, while electrons are free to move:

$$\frac{\partial \vec{B}}{\partial t} = -\vec{\nabla} \times \left\{ \frac{c^2}{4\pi\sigma} \vec{\nabla} \times (e^\nu \vec{B}) + \frac{c}{4\pi en_e} \left[\vec{\nabla} \times (e^\nu \vec{B}) \right] \times \vec{B} \right\}. \quad (3.1)$$

Here, c is the speed of light, the electrical conductivity is defined as $\sigma = e^2 n_e \tau_e / m_e^*$, with n_e being the electron number density, τ_e the relaxation time of the electrons, m_e^* the electron effective mass, and e the fundamental charge. The relativistic factors e^ν come from the Schwarzschild metric, suitable to describe the background structure of the star, assumed fixed during the star's lifetime and obtained by solving the TOV equations for a given equation of state.

The electrical conductivity in the crust lies in the range $\sigma \sim 10^{22} - 10^{25} \text{ s}^{-1}$, orders of magnitude larger than for any terrestrial non-superconductive material. The first term on the right-hand side represents the Ohmic dissipation, and the second term is the nonlinear Hall term. Both terms become larger in the outermost layers of the crust, due to the decreasing density. Therefore, both the Ohmic or Hall timescales vary by many orders of magnitude in depth and across the lifetime of the neutron star, depending on the local conditions.

Recent works study the influence of the expected slow, ionic plastic flow (Beloborodov & Levin 2014; Lander 2016; Lander & Gourgouliatos 2019; Kojima et al. 2022). The net result is that the Hall timescales could be partially slowed down, but the general Hall-dominated behaviour persists for magnetic fields $B \gtrsim 10^{14} \text{ G}$.

The most important effect of the Hall term is to re-distribute the magnetic energy over a wide range of spatial scales. This implies that any purely large-scale field will be partially re-organized, and small-scale magnetic structures will appear. As studied in box simulations (see e.g. one recent example, Brandenburg (2020)), the Hall effect is expected to trigger an avalanche that re-organize any specific initial field topology over a broad range of spatial scales. This is called a Hall cascade. While the stratification and the peculiar shell-like geometry of a neutron star can partially hamper such cascade, there are convincing pieces of evidence from recent 3D simulations of neutron star crust that the Hall cascade can happen (Gourgouliatos et al. 2016; Wood & Hollerbach 2015). These simulations show a persisting plethora of small magnetic structures, visible also by the quite flat spectral magnetic energy distribution and visual features (e.g., Igoshev et al. (2021)). Related to this, simulations with the same *Parody* code show that an initial purely large-scale torodial field quickly develops high-wavenumber perturbations of the magnetic field (Gourgouliatos & Pons 2019). It is the so-called Hall instability. While it is extremely unlikely that nature can ever produce such initial idealized fields, these numerical studies, and their analytically supported outcome, show the natural tendency of a Hall-MHD system to create and maintain small structures.

This reinforces the idea that, even in the absence of a continuous dynamo mechanism and with resistive processes at work, the Hall cascade tends to continuously redistribute energy over a wide range of scale, maintaining a sort of equilibrium spectral distribution.

Additionally, Dehman et al. (2020) proved with 2D simulations how the expected crustal failure rate from magnetars, coming from excessive magnetic stresses, is proportional to the total magnetic energy stored in the crust (or, similarly, on the total intensity of currents circulating in the crust). There is no correlation with the dipolar component alone, which agrees with the sporadic discoveries of low-B magnetars.

Note that most of the 2D and 3D simulations (see Pons & Viganò (2019) and references within, and works by e.g. Gourgouliatos et al. (2016); Gourgouliatos & Hollerbach (2018); De Grandis et al. (2020, 2021); Igoshev et al. (2021)) usually consider an unrealistic (and physically unjustified) topology confined to the crust. This is due to practical reasons,

since the magnetism in the core is still unclear even from a theoretical point of view. The ambipolar diffusion (Goldreich & Reisenegger 1992; Castillo et al. 2017, 2020) should have a role in re-organizing the field, aligning currents and magnetic fields, but the timescales over which this may happen will strongly depend on the so far theoretical unclear effects of the superconductivity over the macroscopic fluid movements. See Gusakov et al. (2020) and references within for the current state of understanding and open questions about the superconducting core evolution. Given the large fundamental uncertainties, it is by now very hard to predict how the topology affects the core magnetic evolution, but it is likely to be much more complicated than the usual twisted-torus plus dipole configurations usually considered in simulations (e.g., Viganò et al. (2021)).

Finally, virtually all magneto-thermal models assume a perfectly potential configuration outside, something in tension with the observational evidence listed above. The better attempts so far to overcome this limitation is to let helicity (i.e., electrical currents) to flow into the magnetosphere, via a non-trivial coupling between interior and exterior (Akgün et al. 2018). A progress in this direction, and the inclusion of Ohmic dissipation in magnetized envelope models (see the review by Potekhin et al. (2015)) will be very helpful to further clarify the formation of bundles and hotspots discussed above.

4. Binary neutron star's mergers

Finally, let us have a look on the magnetic properties during the final stage of a binary neutron star (BNS) system, a hot topic after the GW170817 event. Numerical relativity simulations of merging BNSs have witnessed huge progresses in the last couple of decades, in term of fundamental ingredients like magnetic fields, realistic equations of state and neutrino radiation (see e.g. Shibata (2016); Duez & Zlochower (2019); Shibata & Hotokezaka (2019); Palenzuela (2020) for recent reviews).

Magnetic fields play an important role in the post-merger evolution, since they are connected to the formation of relativistic jets (i.e., to the gamma-ray burst), and possibly in the properties of the ejected matter and the infrared-optical electromagnetic counterpart of the kilonova. See Ciolfi (2020) for a complete review of the magnetic field imprints on mergers.

Since mergers happen when both stars are \sim Gyr-old, their magnetic fields are arguably not larger than the values typically seen in low-mass X-ray binaries: 10^9 G at most. The amplification of magnetic fields soon after merger is potentially due to different MHD instabilities, in particular: the Kelvin-Helmholtz instability (KHI, Kiuchi et al. (2015)), the Rayleigh-Taylor instability (e.g., Skoutnev et al. (2021)), the magneto-rotational instability Balbus & Hawley (1991); Hawley & Balbus (1991); Balbus & Hawley (1998); Siegel et al. (2013); Kiuchi et al. (2014). All of them tend to grow fast on very small scales that cannot be fully captured with the current affordable resolutions. In the last years, the increase of computational resources have allowed longer and longer simulations with higher and higher resolution Kiuchi et al. (2018). Only recently, large-eddy simulations (LESs) have been introduced in the BNS field, by including new terms in the general relativistic MHD equations (Bucciantini & Del Zanna (2013); Palenzuela et al. (2015); Viganò et al. (2020); Aguilera-Miret et al. (2020, 2021); Palenzuela et al. (2021)). While the first of such works aimed at having a by-hand amplification of the magnetic fields, our latest works adopted refined numerical techniques, including high-order reconstruction schemes and a suitable, mathematical sub-grid scale model (the so-called gradient model, Leonard (1975); Müller & Carati (2002); Viganò et al. (2019); Carrasco et al. (2019)).

In particular, in Palenzuela et al. (2021) we showed for the first time the achievement of numerical convergence in terms of saturation in magnetic energy amplification, and evolution of magnetic spectra. Our LESs (see Fig. 4, adapted from Palenzuela et al. (2021)) show that during the first ~ 5 ms after merger, magnetic fields are amplified up

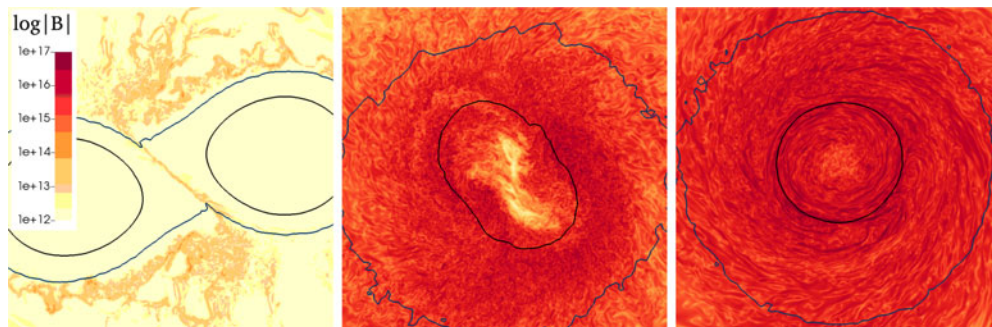


Figure 4. The magnetic field intensity (in Gauss, see scale color) on the orbital plane after 0.5, 3 and 15 ms in a recent high-resolution LES of binary neutron star merger, explained in detail in Palenzuela et al. (2021).

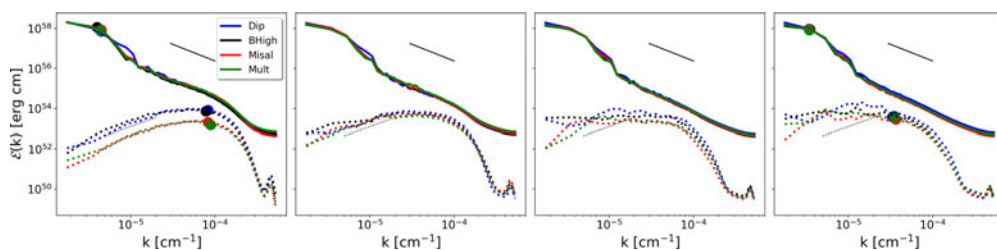


Figure 5. Spectra of the kinetic (solid) and magnetic energy (dashed) at $t = (5, 10, 20)$ ms, given by LES shown in Aguilera-Miret et al. (2021). Different colors correspond to different initial topologies inside each star. The high- k features are numerical artifacts arising from the Fourier transforms of the fields evolved by a finite-difference/finite-volume numerical scheme. The dot points represent the spectra-weighted average wavenumber, corresponding to $2\pi/L$, where L is the typical lengthscale. Adapted from Aguilera-Miret et al. (2021).

to an average intensity of $\sim 10^{16}$ G in the bulk of the remnant, at least three orders of magnitude than its initial value. After that, the average magnetic field intensity saturates and is nearly constant for tens of milliseconds, corresponding to volume-integrated magnetic energies of $\sim 10^{51}$ erg s^{-1} . In the envelope surrounding the remnant, the average magnetic field tends to be about one order of magnitude smaller, $\sim 5 \times 10^{14} - 10^{15}$ G at saturation.

More importantly, the magnetic field is highly turbulent at all stages. Typical kinetic and magnetic spectra are displayed in Fig. 5 at times $t = (5, 10, 20)$ ms, for a range of different LES, as shown in Aguilera-Miret et al. (2021). The distribution over a broad range of scales is evident. The turbulence is initially triggered at the shear layer between the two colliding cores (due to the KHI), and at the low-density layers surrounding the merging stars. The rich fluid dynamics causes the turbulent state to quickly propagate throughout the remnant, in an isotropic, pretty homogeneous way. The spectra of the poloidal and toroidal components are very similar at 5 ms. Equipartition between magnetic and kinetic energy is reached only above certain wavenumber k , which slowly decreases in time. The magnetic field at lower k is compatible with the Kazantsev power law $k^{3/2}$, typical of the kinematic phase of a small-scale dynamo. Looking at the evolution, the poloidal component slightly decreases, while the toroidal component increases, with a slow but steady inverse cascade transferring energy from small to large scales. The linear increase of the toroidal field is compatible with the winding mechanism induced by the differential rotation of the remnant. As discussed in detail in Palenzuela et al. (2021), we don't see clear evidence of magneto-rotational instability, a mechanism that by definition

operates over a smooth, stable, large-scale background field, here completely absent since the first instant after merger. The kinetic spectra, instead, seem to follow the classical hydrodynamic universal slope of Kolmogorov, $\propto k^{-5/3}$, i.e. dominated by large scales. Quantitatively, in our simulation the average length-scale of the magnetic field variation is of the order of \lesssim km, while for the velocity field it is of the order of the remnant size ($\sim 10 - 20$ km).

Recently, we have shown (Aguilera-Miret et al. 2021) how the pre-merger topology of the two neutron stars has no influence on the magnetic field properties of the remnant. As a matter of fact, the dynamo is small-scale dominated and is governed by the MHD turbulence triggered by the KHI. As a consequence, the memory of the weak initial field is lost. This numerical outcome is obtained in presence of accurate enough simulations (in terms of numerical scheme and resolution), and if the pre-merger fields are not unrealistically high. We refer to Aguilera-Miret et al. (2020); Palenzuela et al. (2021); Aguilera-Miret et al. (2021) for further in-depth discussions and details of these simulations.

The bottomline is that the magnetic configuration after a merger is completely turbulent and dominated by small scales during tens of milliseconds. Only at later times a large-scale re-organization of the toroidal field starts to act, and longer simulations are needed to follow-up hundreds of milliseconds. In any case, the small scales will not disappear and represent a fundamental contribution to the total magnetic energy. Any long-living remnant, including newborn millisecond magnetars, will be endowed with an extremely complex magnetic field, where the dipolar component will be a minor fraction of the total energy, similarly to what the core-collapse supernova simulations show, as discussed above.

5. Conclusions

The dipolar assumption in neutron stars' magnetism is reasonable to have a first approximation for the rotational evolution (e.g., Spitkovsky (2006)) and an average field. However, theoretical, numerical and observational considerations point to the fact that a wide range of spatial scales is relevant in term of distribution of magnetic energy. Although this complicates the picture and poses challenges, the dipolar assumption, if used, should be always kept in mind. Small-scale structures and non-potential configurations are likely to be there across all stages of a neutron star's life, in the same way as non-trivial topologies are ubiquitous in astrophysical magnetism in general.

Acknowledgments

DV is funded by the European Research Council (ERC) Starting Grant IMAGINE (grant agreement number 948582) under the European Union's Horizon 2020 research and innovation programme. DV's work was also partially supported by the Spanish program Unidad de Excelencia María de Maeztu CEX2020-001058-M.

References

- Aguilera-Miret R., Viganò D., Carrasco F., Miñano B., Palenzuela C., 2020, *Phys. Rev. D*, 102, 103006
- Aguilera-Miret R., Viganò D., Palenzuela C., 2021, arXiv e-prints, p. arXiv:2112.08406
- Akgün T., Cerdá-Durán P., Miralles J. A., Pons J. A., 2018, *MNRAS*, 481, 5331
- Aurière M., Wade G. A., Silvester J., Lignières F., Bagnulo S., Bale K., Dintrans B., Donati J. F., Folsom C. P., Gruberbauer M., 2007, *A&A*, 475, 1053
- Balbus S. A., Hawley J. F., 1991, *ApJ*, 376, 214
- Balbus S. A., Hawley J. F., 1998, *Reviews of Modern Physics*, 70, 1

- Beloborodov A. M., 2009, *ApJ*, 703, 1044
- Beloborodov A. M., 2011, in Torres D. F. & Rea N. ed., *High-Energy Emission from Pulsars and their Systems Activated Magnetospheres of Magnetars*. p. 299
- Beloborodov A. M., 2012, *ArXiv e-prints*
- Beloborodov A. M., 2013, *ApJ*, 762, 13
- Beloborodov A. M., Levin Y., 2014, *ApJL*, 794, L24
- Beloborodov A. M., Li X., 2016, *ApJ*, 833, 261
- Beloborodov A. M., Thompson C., 2007, *ApJ*, 657, 967
- Bilous A. V., Watts A. L., Harding A. K., Riley T. E., Arzoumanian Z., Bogdanov S., Gendreau K. C., Ray P. S., Guillot S., Ho W. C., et al., 2019, *The Astrophysical Journal Letters*, 887, L23
- Borghese A., Rea N., Coti Zelati F., Tiengo A., Turolla R., 2015, *ApJL*, 807, L20
- Borghese A., Rea N., Coti Zelati F., Tiengo A., Turolla R., Zane S., 2017, *MNRAS*, 468, 2975
- Braithwaite J., Nordlund Å., 2006, *A&A*, 450, 1077
- Braithwaite J., Spruit H. C., 2004, *Nature*, 431, 819
- Brandenburg A., 2020, *ApJ*, 901, 18
- Bucciantini N., Del Zanna L., 2013, *MNRAS*, 428, 71
- Carrasco F., Viganò D., Palenzuela C., Pons J. A., 2019, *MNRAS*, 484, L124
- Castillo F., Reisenegger A., Valdivia J. A., 2017, *MNRAS*, 471, 507
- Castillo F., Reisenegger A., Valdivia J. A., 2020, *MNRAS*, 498, 3000
- Cioffi R., 2020, *General Relativity and Gravitation*, 52, 59
- Cioffi R., Ferrari V., Gualtieri L., Pons J. A., 2009, *MNRAS*, 397, 913
- Cioffi R., Rezzolla L., 2013, *MNRAS*, 435, L43
- Connerney J. E. P., Kotsiaros S., Oliverson R. J., Espley J. R., Joergensen J. L., Joergensen P. S., Merayo J. M. G., Hecceg M., Bloxham J., Moore K. M., Bolton S. J., Levin S. M., 2018, *GRL*, 45, 2590
- Coti Zelati F., Borghese A., Rea N., Viganò D., Enoto T., Esposito P., Pons J. A., Campana S., Israel G. L., 2020, *A&A*, 633, A31
- Coti Zelati F., Rea N., Pons J. A., Campana S., Esposito P., 2018, *MNRAS*, 474, 961
- Cumming A., Macbeth J., 2004, *ApJL*, 603, L37
- De Grandis D., Taverna R., Turolla R., Gnarini A., Popov S. B., Zane S., Wood T. S., 2021, *ApJ*, 914, 118
- De Grandis D., Turolla R., Wood T. S., Zane S., Taverna R., Gourgouliatos K. N., 2020, *ApJ*, 903, 40
- Dehman C., Viganò D., Rea N., Pons J. A., Perna R., Garcia-Garcia A., 2020, *ApJL*, 902, L32
- Duez M. D., Zlochower Y., 2019, *Reports on Progress in Physics*, 82, 016902
- Esposito P., Israel G. L., Zane S., Senziani F., Starling R. L. C., Rea N., Palmer D. M., Gehrels N., Tiengo A., de Luca A., Götz D., Mereghetti S., Romano P., Sakamoto T., Barthelmy S. D., Stella L., Turolla R., Feroci M., Mangano V., 2008, *MNRAS*, 390, L34
- Esposito P., Rea N., Israel G. L., 2021, in Belloni T. M., Méndez M., Zhang C., eds, *Astrophysics and Space Science Library Vol. 461 of Astrophysics and Space Science Library, Magnetars: A Short Review and Some Sparse Considerations*. pp 97–142
- Geppert U., Viganò D., 2014, *MNRAS*, 444, 3198
- Goldreich P., Julian W. H., 1969, *ApJ*, 157, 869
- Goldreich P., Reisenegger A., 1992, *ApJ*, 395, 250
- Götz D., Mereghetti S., Tiengo A., Esposito P., 2006, *A&A*, 449, L31
- Gourgouliatos K. N., Hollerbach R., 2018, *ApJ*, 852, 21
- Gourgouliatos K. N., Pons J. A., 2019, *Physical Review Research*, 1, 032049
- Gourgouliatos K. N., Wood T. S., Hollerbach R., 2016, *Proc. Nat. Acad. Sci. USA*, 113, 3944
- Gusakov M. E., Kantor E. M., Ofengeim D. D., 2020, *MNRAS*, 499, 4561
- Hawley J. F., Balbus S. A., 1991, *ApJ*, 376, 223
- Igoshev A. P., Gourgouliatos K. N., Hollerbach R., Wood T. S., 2021, *ApJ*, 909, 101
- Igoshev A. P., Hollerbach R., Wood T., Gourgouliatos K. N., 2021, *Nature Astronomy*, 5, 145
- Karageorgopoulos V., Gourgouliatos K. N., Contopoulos I., 2019, *MNRAS*, 487, 3333

- Kiuchi K., Cerdá-Durán P., Kyutoku K., Sekiguchi Y., Shibata M., 2015, *Phys. Rev. D*, 92, 124034
- Kiuchi K., Kyutoku K., Sekiguchi Y., Shibata M., 2018, *Phys. Rev. D*, 97, 124039
- Kiuchi K., Kyutoku K., Sekiguchi Y., Shibata M., Wada T., 2014, *Phys. Rev. D*, 90, 041502
- Kochukhov O., 2016, in Rozelot J.-P., Neiner C., eds, Vol. 914, *Lecture Notes in Physics*, Berlin Springer Verlag. p. 177
- Kochukhov O., Papakonstantinou N., Neiner C., 2022, arXiv e-prints, p. arXiv:2201.02554
- Kojima Y., Kisaka S., Fujisawa K., 2022, *MNRAS*
- Lander S. K., 2016, *ApJL*, 824, L21
- Lander S. K., 2021, *MNRAS*, 507, L36
- Lander S. K., Gourgouliatos K. N., 2019, *MNRAS*, 486, 4130
- Lander S. K., Haensel P., Haskell B., Zdunik J. L., Fortin M., 2021, *MNRAS*, 503, 875
- Lander S. K., Jones D. I., 2009, *MNRAS*, 395, 2162
- Leonard A., 1975, *Advances in Geophysics*, 18, 237
- Li X., Levin Y., Beloborodov A. M., 2016, *ApJ*, 833, 189
- Lowes F. J., 1974, *Geophysical Journal*, 36, 717
- Miralles J. A., Pons J. A., Urpin V. A., 2000, *ApJ*, 543, 1001
- Mösta P., Ott C. D., Radice D., Roberts L. F., Schnetter E., Haas R., 2015, *Nature*, 528, 376
- Müller W.-C., Carati D., 2002, *Physics of Plasmas*, 9, 824
- Oliva G. A., Frutos-Alfaro F., 2021, *MNRAS*, 505, 2870
- Palenzuela C., 2020, *Frontiers in Astronomy and Space Sciences*, 7, 58
- Palenzuela C., Aguilera-Miret R., Carrasco F., Ciolfi R., Kalinani J. V., Kastaun W., Miñano B., Viganò D., 2021, arXiv e-prints, p. arXiv:2112.08413
- Palenzuela C., Liebling S. L., Neilsen D., Lehner L., Caballero O. L., O'Connor E., Anderson M., 2015, *Phys. Rev. D*, 92, 044045
- Perna R., Pons J. A., 2011, *ApJL*, 727, L51
- Pons J. A., Perna R., 2011, *ApJ*, 741, 123
- Pons J. A., Rea N., 2012, *ApJL*, 750, L6
- Pons J. A., Viganò D., 2019, *Living Reviews in Computational Astrophysics*, 5, 3
- Potekhin A. Y., Pons J. A., Page D., 2015, *Space Science Rev.*, 191, 239
- Rea N., Coti Zelati F., Viganò D., Papitto A., Baganoff F., Borghese A., Campana S., Esposito P., Haggard D., Israel G. L., Mereghetti S., Mignani R. P., Perna R., Pons J. A., Ponti G., Stella L., Torres D. F., Turolla R., Zane S., 2020, *ApJ*, 894, 159
- Rea N., Esposito P., Pons J. A., Turolla R., Torres D. F., Israel G. L., Possenti A., Burgay M., Viganò D., Papitto A., Perna R., Stella L., Ponti G., Baganoff 2013, *ApJL*, 775, L34
- Rea N., Esposito P., Turolla R., Israel G., Zane S., Stella L., Mereghetti S., Tiengo A., Götz D., Gögüş E., et al., 2010, *Science*, 330, 944
- Rea N., Israel G. L., Esposito P., Pons J. A., Camero-Arranz A., Mignani R. P., Turolla R., Zane S., Burgay M., Possenti A., 2012, *ApJ*, 754, 27
- Rea N., Viganò D., Israel G. L., Pons J. A., Torres D. F., 2014, *ApJL*, 781, L17
- Rea N., Zane S., Turolla R., Lyutikov M., Götz D., 2008, *ApJ*, 686, 1245
- Reboul-Salze A., Guilet J., Raynaud R., Bugli M., 2021a, *A&A*, 645, A109
- Reboul-Salze A., Guilet J., Raynaud R., Bugli M., 2021b, arXiv e-prints, p. arXiv:2111.02148
- Riley T. E., Watts A. L., Bogdanov S., Ray P. S., Ludlam R. M., Guillot S., Arzumanyan Z., Baker C. L., Bilous A. V., Chakrabarty D., Gendreau K. C., Harding A. K., Ho W. C. G., Lattimer J. M., Morsink S. M., Strohmayer T. E., 2019, *ApJL*, 887, L21
- Shibata M., 2016, *Numerical Relativity - 100 Years of general relativity vol. 1*. World Scientific
- Shibata M., Hotokezaka K., 2019, *Annual Review of Nuclear and Particle Science*, 69, 41
- Siegel D. M., Ciolfi R., Harte A. I., Rezzolla L., 2013, *Phys. Rev. D*, 87, 121302
- Skoutnev V., Most E. R., Bhattacharjee A., Philippov A. A., 2021, *ApJ*, 921, 75
- Solanki S. K., 1993, *Space Science Rev.*, 63, 1
- Spitkovsky A., 2006, *ApJL*, 648, L51
- Stenflo J. O., 1978, *Reports on Progress in Physics*, 41, 865
- Sur A., Haskell B., Kuhn E., 2020, *MNRAS*, 495, 1360

- Thompson C., Duncan R. C., 1993, *ApJ*, 408, 194
- Thompson C., Yang H., Ortiz N., 2017, *ApJ*, 841, 54
- Tiengo A., Esposito P., Mereghetti S., Turolla R., Nobili L., Gastaldello F., Götz D., Israel G. L., Rea N., Stella L., Zane S., Bignami G. F., 2013, *Nature*, 500, 312
- Viganò D., Aguilera-Miret R., Carrasco F., Miñano B., Palenzuela C., 2020, *Phys. Rev. D*, 101, 123019
- Viganò D., Aguilera-Miret R., Palenzuela C., 2019, *Physics of Fluids*, 31, 105102
- Viganò D., Garcia-Garcia A., Pons J. A., Dehman C., Graber V., 2021, *Computer Physics Communications*, 265, 108001
- Viganò D., Perna R., Rea N., Pons J. A., 2014, *MNRAS*, 443, 31
- Viganò D., Rea N., Pons J. A., Perna R., Aguilera D. N., Miralles J. A., 2013, *MNRAS*, 434, 123
- Wadiasingh Z., Baring M. G., Gonthier P. L., Harding A. K., 2018, *ApJ*, 854, 98
- Wood T. S., Hollerbach R., 2015, *Phys. Rev. Lett.*, 114, 191101
- Younes G., Kouveliotou C., Jaodand A., Baring M. G., van der Horst A. J., Harding A. K., Hessels J. W. T., Gehrels N., Gill R., Huppenkothen D., Granot J., Göğüş E., Lin L., 2017, *ApJ*, 847, 85